Author(s): Laasonen, K. & Nieminen, Risto M. & Puska, M. J.

Title: First-principles study of fully relaxed vacancies in GaAs

Year: 1992

Version: Final published version

**Please cite the original version:**

Laasonen, K. & Nieminen, Risto M. & Puska, M. J. 1992. First-principles study of fully relaxed vacancies in GaAs. Physical Review B. Volume 45, Issue 8. 4122-4130. ISSN 1550-235X (electronic). DOI: 10.1103/physrevb.45.4122.

# First-principles study of fully relaxed vacancies in GaAs

K. Laasonen, R. M. Nieminen, and M. J. Puska
*Laboratory of Physics, Helsinki University of Technology, SF 02150 Espoo, Finland*
(Received 11 March 1991)

The structural and electronic properties of vacancies in GaAs have been studied using *ab initio* molecular dynamics. The atomic structures of vacancies in different charge states have been optimized by using a simulated-annealing procedure. The neighbor-atom relaxations are modest for neutral, singly negative, and doubly negative Ga vacancies as well as for the neutral As vacancy. In the case of singly and doubly negative As vacancies, very strong inward relaxations are found. These inward relaxations almost recover the fourfold coordination of the neighboring Ga atoms of the vacancy. The analysis of recent positron-annihilation experimental data is discussed in the light of these results.

## I. INTRODUCTION

The electrical and optical properties of semiconductors are to a large extent determined by the point defects these materials contain. Besides different types of impurities, native defects such as vacancies and antisites form the most important and widely studied classes of point defects.[1,2] A characteristic feature of many point defects in semiconductors is the strong coupling between the electronic structure, which depends on the charge state, and the ionic configuration around the defect. For example, the strong lattice relaxation around a vacancy in silicon results in an Anderson "negative-$U$" system, i.e., the vacancy does not bind a single localized electron, but the occupancy of the deep level can be changed from zero to two.[3] Another example is served by the metastable $EL2$ defect in GaAs. In most of the models for $EL2$ atomic displacements occur as a result of electronic excitation.[4–7]

In this work we study the properties of vacancies in GaAs. We solve for the electronic structures and the corresponding ionic positions simultaneously and self-consistently by using the so-called Car-Parrinello (CP) method,[8] which combines density-functional theory[9] (DFT) and molecular dynamics (MD). The CP method is a full *ab initio* method without any empirical parameters. The forces between the atoms are calculated on the basis of DFT, and the ions are then moved accordingly using MD. An important benefit of the CP is also that in the supercell calculations it can handle significantly larger unit cells than the conventional DFT methods. This is essential for avoiding unphysical interactions between vacancies in neighboring supercells.

There have been several studies of GaAs vacancies,[10–13] but none of these has been fully self-consistent with respect to both electronic and ionic degrees of freedom. Either the ionic relaxation is totally neglected,[10,11,13] or only a symmetry-conserving, so-called breathing relaxation, is taken into account.[12] Therefore, our main purpose in this work is to examine the effects due to ionic relaxations in a fully self-consistent way using a large simulation cell. We are especially interested in how the positions of ions neighboring the vacancy change when the charge state of the vacancy changes. This has important consequences for the interpretation of recent positron-annihilation experiments,[14,15] which detect strong relaxation around a native vacancy. The outline of this paper is as follows. In Sec. II we describe the essential features of the CP method and the choice of numerical techniques relevant for this work. The results are presented and discussed in Sec. III, and Sec IV is a short summary.

## II. METHODS

### A. Density-functional approach

In the CP method[8] the electronic structure of the system is described on the basis of the density-functional theory.[9] DFT shows that in order to describe exactly all the ground-state properties of the system it is, in principle, sufficient to know just the ground-state electron density. This makes it possible to map the system of many interacting electrons to an equivalent system of noninteracting electrons, which reduces the computational complexity of the problem enormously. Moreover, the DFT equations have a variational character with respect to the electronic density, i.e., the correct electron density gives the lowest ground-state energy. This enables the solution of the DFT equations iteratively instead of exact diagonalization.

The DFT total energy of a system of interacting atoms can be written in the following form:

$$E_{\mathrm{DFT}}[n(\mathbf{r}),\{\mathbf{R}_I\}]=T[n(\mathbf{r})]+\int d\mathbf{r}\, V_{\mathrm{ext}}(\mathbf{r})n(\mathbf{r}) +\tfrac{1}{2}\int d\mathbf{r}\int d\mathbf{r}'\frac{n(\mathbf{r})n(\mathbf{r}')}{|\mathbf{r}-\mathbf{r}'|} +E_{\mathrm{xc}}[n(\mathbf{r})]+\tfrac{1}{2}\sum_{I\neq J}\frac{Z_I Z_J}{|\mathbf{R}_I-\mathbf{R}_J|}\ , \quad (1)$$

where $n(\mathbf{r})$ is the electron density, $\mathbf{R}_I$ are the instantaneous position vectors of the nuclei, $T$ is the noninteracting kinetic energy for the electrons, $V_{\mathrm{ext}}$ is the Coulomb po-

 

tential due to the nuclei, $E_{xc}$ is the exchange-correlation energy, and $Z_I$ are the nuclear charges. The exact form of $E_{xc}$ is not known, but the local-density approximation (LDA)

$$E_{xc}^{LDA}[n(\mathbf{r})]=\int d\mathbf{r}\, n(\mathbf{r})\varepsilon_{xc}[n(\mathbf{r})] \tag{2}$$

has proven in practice to be a rather reliable approximation.[9] Above, $\varepsilon_{xc}$ is the exchange-correlation energy per electron in a homogeneous electron gas.[16] The other terms besides $E_{xc}$ in Eq. (1) can be calculated exactly so that the accuracy of the LDA determines the accuracy of the calculation. When compared with experiments, LDA has been shown to give very good results for many properties of the systems of interacting atoms, while systematic errors occur for some properties.[9] Equilibrium bond distances between atoms and vibration frequencies belong to the former category, whereas total binding energies and the widths of band gaps in semiconductors and insulators are generally not well reproduced within LDA. In this work we are mainly interested in the structural properties of the systems, and thus LDA should be rather reliable for our purposes.

In order to solve the energy minimization problem it is convenient to express the electronic density as a sum over the single-particle Kohn-Sham orbitals $\psi_i(\mathbf{r})$,

$$n(\mathbf{r})=\sum_i^{occ} f_i|\psi_i(\mathbf{r})|^2 , \tag{3}$$

where $f_i$ are the Fermi-Dirac occupation numbers. The noninteracting-particle kinetic energy can now be written as

$$T[n]=-\tfrac{1}{2}\sum_i^{occ} f_i\psi_i^*(\mathbf{r})\nabla^2\psi_i(\mathbf{r}) . \tag{4}$$

The single-particle orbitals can be solved from the Kohn-Sham equations

$$H\psi_i(\mathbf{r})=e_i\psi_i(\mathbf{r}) , \tag{5}$$

where

$$H=-\tfrac{1}{2}\nabla^2+V_{ext}(\mathbf{r})+\int d\mathbf{r}'\frac{n(\mathbf{r}')}{|\mathbf{r}-\mathbf{r}'|}+\frac{\delta E_{xc}^{LDA}[n]}{\delta n(\mathbf{r})} . \tag{6}$$

This Hamiltonian $H$ depends on the single-particle orbitals $\psi_i$ through the electron density $n(\mathbf{r})$, which calls for a self-consistent solution.

### B. Pseudopotentials and plane waves

The next approximations are to deal with the valence electrons only in Eq. (1) and to use pseudopotentials[17] to describe the effects of tightly bound core electrons. Usually the cores play only a small role in the formation of the chemical bonds between atoms, and therefore this so-called frozen-core approximation is adequate.[18] Within these approximations $n(\mathbf{r})$ and $Z_I$ in Eq. (1) have to be reinterpreted as the pseudo-valence-electron-density and the ionic charge, respectively. We use the norm-conserving nonlocal pseudopotentials by Bachelet, Hamann, and Schlüter[19] (BHS). For numerical convenience we use a separable form for the nonlocal components as introduced by Kleinman and Bylander[20] (KB). The KB scheme can have, due to numerical instabilities, some unfavorable features.[21] Namely, it is possible that there exist spurious states in the band structure, e.g., states, which have more nodes but a lower energy than the physical state. The existence of these spurious states depends strongly on the choice of the pseudopotential parameters. Therefore we do not use for GaAs the original parameters by Bachelet, Hamann, and Schlüter[19] but an equivalent set which should be free of these spurious states.[22]

In the pseudopotential approximation it is possible to use the plane-wave (PW) expansion for the single-particle orbitals. Thus,

$$\psi_i(\mathbf{r})=\sum_{\mathbf{G}} C_i(\mathbf{G})\exp(i\mathbf{G}\cdot\mathbf{r}) , \tag{7}$$

where $G$'s are the reciprocal lattice vectors for the superlattice and $C_i(\mathbf{G})$'s are the corresponding Fourier coefficients. We include in this expansion PW's up to a certain cutoff $\mathbf{G}_{max}$, which is determined by the numerical accuracy requirement. Notice that we calculate $\psi$'s only for the $\Gamma$ point ($\mathbf{k}=\mathbf{0}$) in the Brillouin zone of the super lattice. This restriction is motivated by the fact that the unit cell is so large that band dispersion is small (see below). The use of the $\Gamma$ point only allows us to restrict to real eigenfunctions (in $\mathbf{r}$ space), which saves both computing time and memory. In fact, multiple-$\mathbf{k}$-point calculations are hardly feasible even with present supercomputer resources.

The use of PW's has many desirable features. Firstly, the PW's are very fast to handle using the fast Fourier transformation (FFT). This makes the computational work in the iterative diagonalization algorithm (see below) to scale as $M\ln M$, where $M$ is the number of PW's. Secondly, the forces between atoms can be calculated directly and very accurately, and no corrections[23] to a numerical implementation of the Hellman-Feynman theorem[24] are needed. Thirdly, the PW basis has a uniform accuracy throughout the whole supercell and does not have the overcompleteness problems that are typical of localized (e.g., Gaussian) basis sets. This guarantees that an increase of the number of PW's systematically brings the results closer to the limiting values.

The main drawback of the PW's is that in order to describe accurately rapid variations of the one-particle wave functions, the number of PW's needed can be very large, especially when the pseudopotential is strong. Even when using the relatively soft BHS-type pseudopotentials, most of the first-row atoms (such as O) or transition and nobel metals (such as Cu) cannot be treated with PW's, except in very small systems. Other pseudopotentials[25] are now available, which seem very promising in describing both the first-row[26] and the transition-metal atoms. The CP method is also essential in the sense that the huge amount of PW's often necessary would make it impossible to use conventional diagonalization routines, which usually scale like $M^3$. In the present work the PW basis is used together with the *ab initio* pseudopotentials

of Stumpf, Gonze, and Scheffler.[22]

In dealing with charged vacancies and other defects in semiconductors, one has to be careful with the long-range Coulomb interaction. In order to avoid unphysical situations the total charge of the simulation supercell has to be zero. In this work we compensate the extra or missing (relative to the neutral vacancy) electron charge on the localized deep levels at the vacancy with a rigid background charge, which is uniformly spread over the whole simulation cell to compensate for any long-range Coulomb effects (i.e., it does not affect exchange and correlation). This could, in principle, cause some systematic errors in our results, but as long as the simulation cell is large compared to the size of the vacancy and as long as the deep-level wave functions are well localized, this background effect is expected to be quite small.

### C. Molecular dynamics

The idea of the CP method is to consider the total DFT energy [Eq. (1)] as a many-dimensional classical potential with the ionic positions $R_I$ and the Fourier components $C_n(\mathbf{G})$ of the electron wave functions as variables[8,27] in a global minimization (iterative diagonalization) procedure. Then one writes an effective Lagrangian in which the orthogonality constraints between the eigenfunctions are treated by using the technique of Lagrange multipliers:

$$\mathcal{L}=\tfrac{1}{2}\sum_{i,\mathbf{G}}\mu|\dot{C}_i(\mathbf{G})|^2+\tfrac{1}{2}\sum_I M_I\dot{\mathbf{R}}_I^2-E^{\mathrm{DFT}}[C_i,\mathbf{R}_I] + \sum_{i,j}\Lambda_{ij}(\langle C_i|C_j\rangle-\delta_{ij}) . \tag{8}$$

Above, $\mu$ is a fictitious mass parameter for the "kinetic" energy of the electronic degrees of freedom, $M_I$ are the physical masses of the ions and $\Lambda_{ij}$ are the Lagrange multipliers. The last term in Eq. (8) is the orthogonality constraint, with

$$\langle C_i|C_j\rangle=\sum_{\mathbf{G}}C_i^*(\mathbf{G})C_j(\mathbf{G}) . \tag{9}$$

From the classical Lagrangian of Eq. (8) one can derive the classical equations of motions for both the electronic and ionic degrees of freedom as

$$\mu\ddot{C}_i(\mathbf{G})=-\frac{\delta E^{\mathrm{DFT}}}{\delta C_i(\mathbf{G})}+\sum_j\Lambda_{ij}C_j(\mathbf{G}) , \qquad M_I\ddot{\mathbf{R}}_I(\mathbf{G})=-\frac{\delta E^{\mathrm{DFT}}}{\delta\mathbf{R}_I} . \tag{10}$$

When the plane-wave basis set is used the derivation with respect to ionic positions can be made directly, without using the Hellman-Feynman theorem. The Lagrange multipliers have been evaluated in this work by using the iterative method described in Ref. 27.

The Born-Oppenheimer (BO) surface is the minimum of $E^{\mathrm{DFT}}$ with respect to the electronic degrees of freedom, i.e.,

$$\Phi[\{\mathbf{R}_I\}]=\min_{\{C_i\}}E^{\mathrm{DFT}}[C_i,\mathbf{R}_i] . \tag{11}$$

The BO potential-energy surface defines the true dynamics of the ions, but the second-order temporal dynamics manages to keep the electronic states remarkably close to the BO surface without extra minimization steps, provided that $\mu\ll M_I$. In the case of insulators and semiconductors the total energy, calculated with the CP method, stays very close to the BO surface even for several thousands of time steps.[28]

### D. Numerical considerations

In the GaAs simulations we use a cubic supercell with periodic boundary conditions. This simulation cell contains 64 or 63 atoms for the perfect lattice and for the lattice with a vacancy, respectively. For the pseudopotentials we use the *sp* nonlocality for both Ga and As with the cutoff parameters $c_l(s)=1.5$ and $c_l(p)=1.7$ for both Ga and As.[22] The energy cutoff for the plane-wave expansion is 13 Ry, which corresponds to about 4000 PW's per eigenstate. With these numerical parameters, calculations for the perfect GaAs lattice show that the lattice constant of $a=10.67a_0$ minimizes the total energy. This is very close to the experimental value of $10.68a_0$.[29] We have also made convergence tests by studying in the above-defined simulation cell single As and Ga atoms and $As_2$, $Ga_2$, and GaAs dimers with different energy cutoffs. These results are also well converged at the cutoff of 13 Ry. Since the calculations are spin compensated, the quantitative results for the dimers cannot be compared with experiment. In the dynamical simulations used to find the minimum-energy atomic positions the time step is 5.7 a.u. ($=1.7\times10^{-16}$ s). The value of the electronic mass parameter $\mu$ is 400 a.u., whereas the masses used for the ions are between 2 and 10 amu.

In order to initiate the defect calculations we first calculate the electronic structure for bulk GaAs using the steepest descent (SD) method for the electronic degrees of freedom ($C_i$) only. Therefore we remove one atom from the center of the simulation cell and solve for the new electronic structure. Then we let all the atoms move according the forces derived from Eq. (8) and the equations of motion [Eq. (10)]. In order to find atomic coordinates corresponding to the local energy minima we use both a simulated annealing (SA) process and the normal steepest descent method. In the SA process we slowly reduce the ionic kinetic energy of the system by scaling the fictitious velocities $\dot{C}_i(\mathbf{G})$. In the beginning of simulations SA is much faster than the SD method, but close to the minimum the SD method becomes more effective. The effectiveness of both SA and SD can be increased by replacing the physical masses of the ions with some fictitious, much smaller masses. With SA we have used masses of 5–10 amu and with SD masses of 2–3 amu. Combining the SA and SD methods one can rather effectively find the minimum configuration of the atoms. If possible, we use as a starting point for a new charge state of a vacancy the relaxed ionic configuration for a charge state of the vacancy previously treated. This naturally saves plenty of computing work if the new configuration is close to the old one.

TABLE I. Single-particle eigenvalues (in eV) at some selected **k** points for bulk GaAs. The second column gives the present results and the third column contains the theoretical values of Ref. 30 obtained by using the *sp* nonlocal pseudopotentials. The fourth column contains the experimental results quoted in Ref. 31.

| **k** | Present | Ref. 30 | Experiment |
|---|---|---|---|
| $\Gamma_1$ | −12.43 | −12.56 | −13.1 |
| $L_1$ | −10.88 | −10.90 | −11.24 |
| $X_1$ | −10.17 | −10.14 | −10.75 |
| $X_3$ | −6.72 | −6.72 | −6.70 |
| $L_1$ | −6.55 | −6.54 | −6.70 |
| $X_5$ | −2.56 | −2.59 | −2.80 |
| $L_3$ | −1.06 | −1.09 | −1.30 |
| $\Gamma_{15}$ | 0 | 0 | 0 |
| $\Gamma_1$ | 0.7 | 0.62 | 1.42 |

## III. RESULTS AND DISCUSSION

The band structure obtained for the perfect GaAs lattice is compared with the results of similar calculations by Zhang *et al.*[30] and with experiments in Table I. The eigenvalues we obtained are very close to the values in Ref. 31. The maximum difference is less than 0.15 eV. The calculated band gap is about 0.7 eV, which is due to LDA much smaller than the experimental value of 1.52 eV.

In the following we analyze for each vacancy the ionic relaxation and the electronic structure. The ionic relaxation is divided into three components: the breathing mode and the two components of the pairing mode. These modes are shown schematically in Fig. 1. The breathing mode incorporates the inward or outward relaxation of the system and it describes in an average sense the (open) volume change at the vacancy. The pairing-mode components describe the deviation from pure radial (breathing-mode) relaxation. The electronic structure is analyzed by making contour plots of charge densities and selected wave functions. Moreover, the single-particle eigenvalues are compared with results obtained by other similar calculations.

When an ideal vacancy is created in the perfect GaAs lattice, the dangling $sp^3$ bonds hybridize and form bonding and antibonding states. If the $T_d$ lattice symmetry is conserved, the antibonding states belong to the threefold-degenerate $T_2$ representation and form deep localized states in the energy gap. A symmetry-breaking relaxation connected with the Jahn-Teller effect lifts the spatial degeneracy. The bonding states belong to the nondegenerate $A_1$ representation and they lie within the valence band. The $T_2$ states are $p$ like and the $A_1$ state is $s$ like with respect to the vacancy site. Including the spin degeneracy, six electrons can occupy the $T_2$ states, while two electrons can go into the $A_1$ state. The repulsive potential due to the Ga or As vacancy pushes six (degenerate, including spin) electron states out of the valence band. In the case of the Ga vacancy (As vacancy) only three (five) valence electrons are removed with the Ga atom (As atom), and therefore the neutral Ga vacancy (As vacancy) has three (one) electrons in the localized deep levels. Due to the larger number of removed electrons, the As vacancy is a stronger repulsive perturbation than the Ga vacancy. This is reflected in the fact that in the case of the As vacancy the deep levels lie in the band gap close to the conduction-band minimum, whereas the deep levels of the Ga vacancy are just above the valence band edge.[10,11,13]

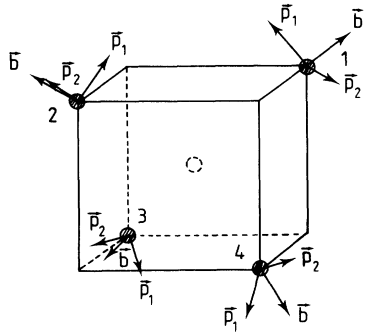


| | $\vec{b}$ | $\vec{p}_1$ | $\vec{p}_2$ |
|---|---|---|---|
| 1: | $(1,1,1)/\sqrt{3}$ | $(-1,-1,2)/\sqrt{6}$ | $(1,-1,0)/\sqrt{2}$ |
| 2: | $(-1,-1,1)/\sqrt{3}$ | $(1,1,2)/\sqrt{6}$ | $(-1,1,0)/\sqrt{2}$ |
| 3: | $(-1,1,-1)/\sqrt{3}$ | $(1,-1,-2)/\sqrt{6}$ | $(-1,-1,0)/\sqrt{2}$ |
| 4: | $(1,-1,-1)/\sqrt{3}$ | $(-1,1,-2)/\sqrt{6}$ | $(1,1,0)/\sqrt{2}$ |

FIG. 1. The different projection vectors of the relaxations. The arrows pointing outwards from the vacancy (**b**) are the breathing-mode components. The arrows $\mathbf{p}_1$ are the pairing mode components and the arrows $\mathbf{p}_2$ are the vectors orthogonal to the previous two.

### A. Ga vacancies

We study the Ga vacancy in the three different charge states, i.e., $V_{Ga}$, $V_{Ga}^-$, and $V_{Ga}^{2-}$ containing three, four,

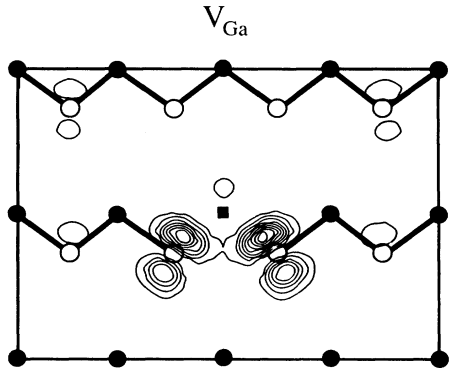


FIG. 2. The electronic density corresponding to the highest state of $V_{Ga}$. The figure shows a region of the (110) plane limited by the borders of the simulation cell. The plane is chosen so that there is a bond between the As atoms neighboring the vacancy. The contour spacing is one tenth of the maximum value. The black dots are the Ga atoms and the white ones are the As atoms. The vacancy is marked with a black square.

TABLE II. Relaxations and deep-level eigenenergies ($\varepsilon_{loc}$) for different vacancies in GaAs. The breathing and pairing mode relaxations (See Fig. 1) are given in percent of the bulk bond distance in GaAs. For the breathing mode the negative (positive) sign denotes inward (outward) relaxation. $\tau$ is the experimental positron lifetime connected with the vacancy.

| Vacancy | Breathing (%) | Pairing 1 (%) | Pairing 2 (%) | $\varepsilon_{loc}$ (eV) | | | $\tau$ (ps) |
|---|---|---|---|---|---|---|---|
| $V_{Ga}$ | −3.9 | 1.3 | 0.9 | 0.56 | 0.59 | | 260[a] |
| $V_{Ga}^{-}$ | −2.9 | 1.2 | 0.2 | 0.57 | 0.58 | | |
| $V_{Ga}^{2-}$ | −3.8 | 0.9 | 0.1 | 0.58 | 0.59 | 0.62 | |
| $V_{As}^{+}$ | +3.0 | 0.0 | 0.0 | | | | |
| $V_{As}$ | +2.0 | 0.6 | 0.0 | 1.41 | | | 295[b] |
| $V_{As}^{-}$ | −16.4 | 17.0 | 0.0 | 0.65 | | | 258[b] |
| $V_{As}^{2-}$ | −17.4 | 15.6 | 0.7 | 0.59 | 12.9 | | |

[a]References 36 and 37.
[b]References 14 and 15.

and five electrons on the deep levels, respectively. The results for the different relaxation components and the eigenvalues of the localized deep levels states are presented in Table II. In the symmetry-conserving breathing mode all the negative vacancies relax inwards. The relaxations are small, a few percent of the equilibrium bond distance. The pairing mode components are even smaller. They are negative in sign, which indicates that the nearest As atoms of the vacancy get pairwise closer to each other, in addition to the reduction in distance between them due to the inward breathing relaxation. However, all the atomic movements are small (the next-nearest neighbors hardly move at all) so that the relaxation is very well contained inside the simulation cell.

According to Table II the deep levels due to the Ga vacancies are below the middle of the experimental band gap. The deep levels (two for $V_{Ga}$ and $V_{Ga}^{-}$, three for $V_{Ga}^{2-}$; our calculations are spin-restricted) are nearly degenerate, the energy splittings being of the order of 0.01 eV. The electron density corresponding to the highest state of $V_{Ga}$ is plotted in Fig. 2. The wave function is mainly $p$ like about the As sites. The wave function of the third deep level in $V_{Ga}^{2-}$ is very similar to that of the second deep level in $V_{Ga}$ (Fig. 2) reflecting the near degeneracy of the deep levels in the Ga vacancy. The deep states have some tendency to spread along the atomic chains, which means that these states are nearly degeneracy also with the top of the valence band. However, the localization to the vacancy region is high enough in the comparison with the extent of the simulation cell, so that the interaction of a vacancy with its periodic replicas is expected to be small.

### B. As vacancies

The As vacancy is studied in four different charge states, $V_{As}^{+}$, $V_{As}$, $V_{As}^{-}$, and $V_{As}^{2-}$, containing zero, one, two, and three electrons on the deep levels, respectively. The results of the calculations are presented in Table II and in Figs. 3–5. For the positively charged and neutral As vacancy the breathing-mode relaxation is rather small, 2–3 % outwards. The pairing-mode relaxation is also small and similar to the case of the Ga vacancy. In the positively charged vacancy no Jahn-Teller distortion is operative. For the neutral vacancy with a single electron the distortion is also small. We argue that this is due to the delocalized nature of the $T_2$ state. As can be seen from Fig. 3, the singly occupied deep state at the neutral As vacancy is spread out spatially. The delocalized nature reflects that this state is in fact in the energy region of the conduction band in the *perfect lattice.*

According to our calculations the neutral As vacancy deep level is 1.4 eV above the valence-band edge and the width of the band gap is about 0.7 eV. (Note that within the single-**k**-point approximation level filling can be unambiguously done by occupying the discrete energy levels in succession.) In order to treat this state more accurately one should avoid the artificial interactions between unit cells, which result in a small but finite band dispersion for the localized defect states. Similarly to our case of the neutral As vacancy, the calculations for a neutral Si vacancy with a smaller 54-atom supercell have been found to suffer from interactions between supercells.[32] One could use a larger simulation cell in the su-

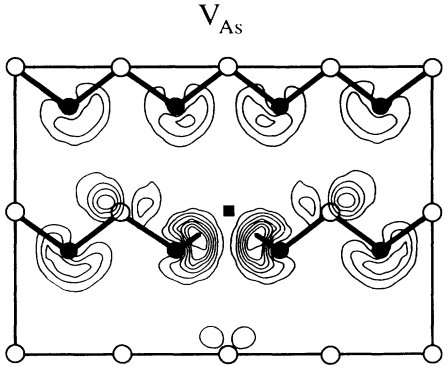


FIG. 3. The electronic density corresponding to the highest state of $V_{As}$. The figure shows a region of the (110) plane limited by the borders of the simulation cell. The plane is chosen so that there is no bond between the Ga atoms neighboring the vacancy. The contour spacing is one tenth of the maximum value. The symbols are the same as in Fig. 2.

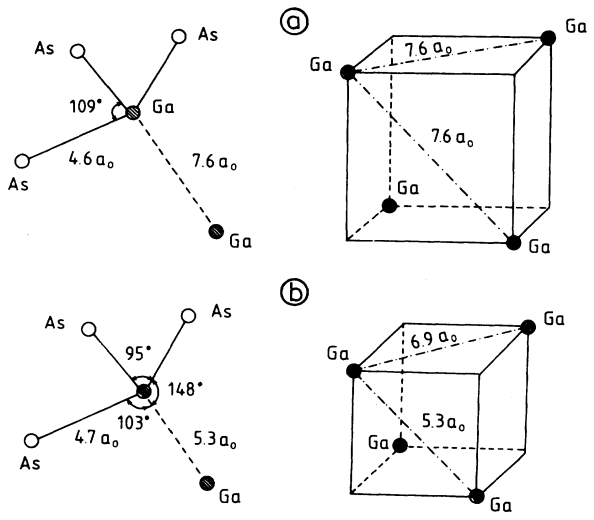


FIG. 4. (a) One of the four nearest Ga atoms of the $V_{As}^-$ in the unrelaxed case. The bond distances and the bond angles are shown in the figure. The cube formed by the four nearest Ga atoms is shown on the right-hand side of the figure. (b) As in (a), but after relaxation. The parallelpiped formed by the four nearest Ga atoms is shown on the right-hand side of the figure.

percell method or, alternatively, use Green's-function embedding methods. Moreover, in all methods one should avoid the problems due to the too narrow band gap, for example, by using the scissors-operator technique discussed by Baraff and Schlüter.[33] This is because even according to the Green's-function methods the deep level at the neutral As vacancy is above the bottom of the conduction-band calculated in LDA.[10,13] Unfortunately, in our case improvements are hardly possible because the next suitable supercell would contain 128 atoms (and 512 electrons), which is beyond the available computer resources. However, we believe that the structural properties obtained are reliable in spite of these problems because they are determined by the total energy and the electron density, which are the relevant physical quantities in DFT. The total-energy differences for different lattice relaxations are of the order of 0.1–0.3 eV. While this is similar in magnitude with the estimated band dispersion due to the supercell, experimentation[34] with multiple **k** points using a tight-binding model[35] shows that the total energy is not sensitive to the level width. Moreover, Wang, Chang, and Ho[36] have shown using the tight-binding method for Si that the results for defect formation energies and relaxations do not significantly change for supercell sizes between 64 and 512 atoms.

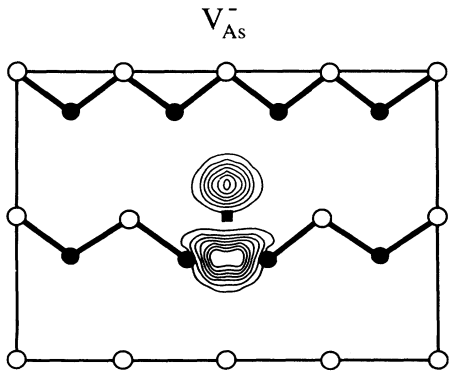


FIG. 5. The electronic density corresponding to the highest state of $V_{As}^-$. The plane is chosen so that their is a bond between the Ga atoms neighboring the vacancy. The contour spacing is one tenth of the maximum value. The symbols are the same as in Fig. 2.

Unlike in case of the Ga vacancy the change of charge-state changes dramatically the structure of the As vacancy. When one electron is added to $V_{As}$ and $V_{As}^-$ is created, the breathing-mode relaxation goes from +2 to −16% (Table II). At the same time strong pairing-mode relaxations appear. Moreover, the energy level of the localized state is substantially lowered, i.e., from 1.4 to 0.6 eV above the top of the valence band. This makes the Jahn-Teller distortion large. It is interesting to recognize that the relaxation almost recovers the fourfold coordination of the Ga atoms nearest neighbors to the vacancy. This is illustrated in Fig. 4. In the ideal case the four Ga atoms next to the vacancy form a tetrahedron, which can be completed to a cube as shown. The distance between two adjacent Ga atoms is $7.6a_0$. In the relaxation the cube deforms to a tetragon, in which the distances between the adjacent Ga atoms are $5.4a_0$ and $6.9a_0$. As a result the Ga atoms have almost gained a fourfold coordination. The electron density plots for the deep state in Figs. 3 and 5 show the formation of a strong bond between the closest Ga atoms. Figure 3 gives the electron density corresponding to the deep level at the neutral As vacancy. The bond between the two Ga atoms is very weak. Figure 5 shows that in the case of the negative vacancy there are clear bonds between the closest Ga atoms.

The doubly negative As vacancy is very similar to the $V_{As}^-$. The last electron added goes to a state with a different symmetry as the strongly bonding state in Fig. 5. The highest state is not well localized, and therefore it does not disturb the well localized bonds between the closest Ga atoms.

### C. Discussion

In the case of the Ga vacancy, the dangling bonds do not show a tendency to form bonds between the As atoms around the vacancy in any charge state. The small inward relaxation can be understood as a very weak bonding between As atoms surrounding the vacancy or a weakening of the back bonds between these As atoms and the neighboring Ga atoms. The inward relaxation does not increase monotonically as a function of the number of electrons in the localized states as one would naively expect from the increase of negative "charge" inside the vacancy. However, the changes between the charge states are very small and a highly accurate calculation of the relaxation is difficult because the equipotential surfaces are

very flat.

The positive and neutral As vacancies relax outwards. In the neutral case, there is only one electron occupying the localized states formed by the dangling bonds in a rather large vacancy. This additional "negative charge" is not enough to compensate the strengthening of the back bonds due to the lowering of the coordination number of the Ga atoms nearest to the vacancy. The second localized electron in $V_{As}^{-}$ goes to the same symmetry state as the first one. This strengthens the bonds between the Ga atoms and according to our results there is a huge change in the relaxation. It is interesting to note that in the case of a vacancy in Si the lattice relaxation and the associated total energy lowering, when adding the second localized electron, are so large that the vacancy with one localized electron $V_{Si}^{+}$ is unstable.[3] This is the well-known Anderson "negative-$U$" system. Unfortunately due of the compensating electronic background the zero level of the total energy will change with the charge of the system. This makes it difficult to compare the relative energies of different charge states.

The electronic structures for the *unrelaxed* neutral Ga and As vacancies have been studied by Bachelet, Baraff, and Schlüter[10] by the pseudopotential Green's-function method. We can make qualitative comparisons of their results with ours for the Ga vacancy in all charge states and also for the neutral As vacancy. These Green's-function calculations give unique values for the localized energy levels, whereas the supercell method always results in some band dispersion, which makes strictly quantitative comparisons difficult. The charge densities and the positions of the deep energy levels in the band gap are in good qualitative agreement. Bachelet, Baraff, and Schlüter[10] give the positions of 0.06 and 1.08 eV above the top of the valence band for the deep levels in the neutral Ga and As vacancies, respectively. Puska *et al.*[13] have obtained with the Green's-function technique corresponding to the linear-muffin-tin orbital (LMTO) method within the atomic spheres approximation (ASA) similar results, 0.06 and 1.13 eV for the neutral Ga and As vacancy, respectively. Our corresponding values are somewhat higher in energy, i.e., 0.56 and 1.4 eV. The interactions between neighboring vacancies (band dispersion) in our calculations may raise the localized energy levels relative to the Green's function calculations. When the charge state of the vacancy becomes more negative the deep level raises according to Puska *et al.*[13] due to the increased Coulomb repulsion between the localized electrons. This tendency is not reproduced in our calculation because the effects due to the lattice relaxation compensate and even overcome the Coulomb repulsion.

The only other calculation of vacancy relaxation in GaAs that is known to us is by Scheffler and Scherz.[12] They have studied the singly negative Ga vacancy and the neutral As vacancy allowing only a breathing-type relaxation. For $V_{Ga}^{-}$ and $V_{As}^{0}$ they report the breathing-mode relaxation of $+2\%$ and $-3\%$, respectively. These relaxations are in the opposite directions as our results, but the main conclusion from both calculations is that the relaxations in these cases are small in magnitude. The deep level positions obtained by Scheffler and Scherz,[12] about 0.1 eV for $V_{Ga}^{-}$ and 1.25 eV $V_{As}^{0}$ are in good agreement with the results discussed above.

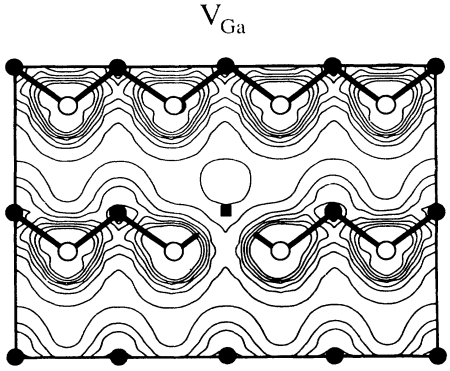


FIG. 6. The total valence electron density corresponding to $V_{Ga}$. The rapid variations of the density inside the As-ion cores are not shown. The first contours surrounding the interstitial regions correspond to the electron density of $0.006a_0^{-3}$ and the contour spacing is $0.01a_0^{-3}$. Note that there is a local maximum just above the center of the vacancy. The figure shows the same (110) plane as Fig. 2. The symbols are the same as in Fig. 2.

It is interesting to compare the present results with the positron lifetime measurements for GaAs.[37,38,14,15] The positron annihilation rate is proportional to the effective electron density seen by the positron. Positrons are trapped by vacancies in solids because of the reduction of the repulsion due to positive ion cores. In semiconductors, however, this trapping does not occur for positively charged vacancies, due to the long-range Coulomb repulsion. In the lifetime measurements, positron trapping at vacancies is seen as an appearance of a long-lifetime component in the spectrum. The lifetime increases because the average electron density seen by a positron trapped by a vacancy is smaller than that for a positron delocalized in the perfect crystal. According to the present understanding[13,39,40] the lifetime related to the vacancies is sensitive to the open volume seen by the positron. The calculations[39] also show that the positron lifetime

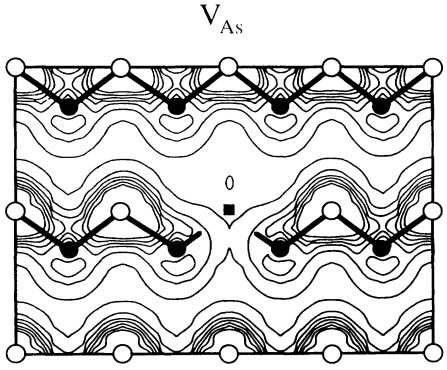


FIG. 7. The total valence electron density corresponding to $V_{As}$. The rapid variations of the density inside the As-ion cores are not shown. The figure shows the same (110) plane as Fig. 5. The symbols are the same as in Fig. 2 and the contour spacing as in Fig. 6.

changes with the breathing relaxation, but pure tetragonal and trigonal relaxations do not appreciably affect the positron lifetime. Moreover, the positron lifetime is not directly sensitive to the charge state of the trap, i.e., if the charge-state changes but the change in relaxation is not taken into account, the positron lifetime remains nearly unaltered.[13,40] This insensitivity reflects the relatively delocalized nature of the deep electron states at vacancies and the fact that the positron has the tendency to follow the electron charge transfer. Therefore the positron lifetime measurements are an efficient tool to monitor the open volume, in particular the amplitude of the breathing relaxation, at the vacancies.

The measured positron lifetimes associated with different vacancies in GaAs are collated in Table II. For the Ga vacancies, only one lifetime value of 260 ps has been seen.[37,38] Also according to our calculations only one component is to be expected, because the relaxations in different relevant charge states are very similar. In the case of the As vacancy it has been found that the positron lifetime decreases from the value of 295 ps to the value of 258 ps when the charge of the As vacancy decreases by one.[14,15] This is a very large change in the positron lifetime (the positron lifetime for the perfect GaAs lattice is 230 ps) and indicates a strong inward relaxation of the As vacancy. Recently, using indirect experimental arguments the 295 ps and 258 lifetime components have been associated with $V_{As}^{0}$ and $V_{As}^{-}$, respectively.[15] This assignment is in complete qualitative agreement with our results, which show that the change in the breathing-mode relaxation between these states is large, 18.5%. Moreover, this is in accord with theoretical calculations, which estimate that the amount of relaxation needed to produce the experimental lifetime difference is about 15%.[40] On the other hand, in order to reproduce the *absolute* lifetime values with the present positron state calculation methods the relaxations of the vacancies should be more in the outward direction.[39,40] Thus, the present results for the electronic and atomic structures for the vacancy defects indicate a need for a reexamination of the basic approximations, nominally the inclusions of the many-body effects, in the lifetime calculation for positrons in shallow semiconductor traps. However, the relatively large difference [260 ps vs 295 ps (Refs. 37, 38, and 14)] in the positron lifetimes between the neutral Ga and As vacancies can be understood on the basis of the total valence electron densities shown in Figs. 6 and 7. One can see that the open volume for the As vacancy is larger than for the Ga vacancy. Total valence electron density for $V_{As}^{-}$ is shown in Fig. 8. The open volume is clearly reduced from that for the neutral vacancy in Fig. 7.

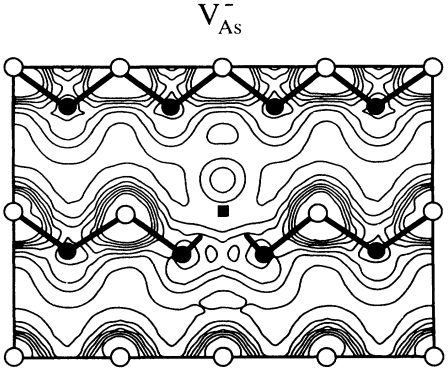


FIG. 8. The total valence electron density corresponding to $V_{As}^{-}$. The rapid variations of the density inside the As-ion cores are not shown. The figure shows the same (110) plane as Fig. 5. The symbols are the same as in Fig. 2 and the contour spacing as in Fig. 6.

## IV. SUMMARY

We have performed state-of-art calculations for the electronic and ionic structures of vacancies in GaAs. Studying different charge states we find that the changes in the ionic relaxations are usually rather small, but when going from $V_{As}^{0}$ to $V_{As}^{-}$ a very large inward relaxation takes place with a strong pairing of the Ga atoms nearest to the vacant site. This finding shows that the ionic relaxations are coupled in a crucial way with the electronic structure of defects in GaAs, and the understanding of the properties of GaAs is not possible without a simultaneous optimization of electronic and ionic degrees of freedom. This conclusion has been drawn also in the case of a recent theoretical model for the $EL2$ defect in GaAs.[4] In this work we have briefly discussed the ionic relaxations obtained parallel with the results from positron lifetime spectroscopy, which is a sensitive tool to detect vacancy defects and the open volumes associated with them. The present results show that the calculated changes in the relaxations (open volume) correlate very well with observed lifetimes. The largest effect is assigned to the transition between the neutral and singly negative As vacancy.

## ACKNOWLEDGMENTS

We would like to thank P. Hautojärvi and K. Saarinen for many useful discussions about the results of positron lifetime experiments. One of us (K.L.) would like to thank SISSA and its staff for their hospitality. He is especially grateful to Professor Roberto Car for his help with, and explanations of, the Car-Parrinello method and related aspects. This work has been supported in part by a grant from the Academy of Finland. We also acknowledge the generous supercomputer resources made available through Center for Scientific Computing (CSC) in Espoo.

[1]Proceedings of the 14th International Conference on Defects in Semiconductors, Paris, 1986, edited by H. J. von Bardeleben [Mater. Sci. Forum **10-12**, 1986)].
[2]Proceedings of the 15th International Conference on Defects in Semiconductors, Budapest, 1988, edited by G. Ferenczi [Mater. Sci. Forum **38-41** (1989)].
[3]G. A. Baraff, E. O. Kane, and M. Schlüter, Phys. Rev. B. **21**, 5662 (1980).
[4]J. Dabrowski and M. Scheffler, Phys. Rev. B **40**, 10 391 (1989); D. J. Chadi and K. J. Chang, Phys. Rev. Lett. **60**, 2187 (1988).
[5]G. A. Baraff and M. Schlüter, Phys. Rev. Lett. **55**, 2340 (1985).
[6]H. J. von Bardeleben, D. Stievenard, D. Deresmes, A. Huber, and J. C. Bourgoin, Phys. Rev. B **34**, 7192 (1986).
[7]J. F. Wager and J. A. Van Vechten, Phys. Rev. B **35**, 2330 (1987).
[8]R. Car and M. Parrinello, Phys. Rev. Lett. **55**, 2471 (1985).
[9]For a recent review, see, e.g., R. O. Jones and O. Gunnarson, Rev. Mod. Phys. **61**, 689 (1989).
[10]G. B. Bachelet, G. A. Baraff, and M. Schlüter, Phys. Rev. B **24**, 915 (1981).
[11]G. A. Baraff and M. Schlüter, Phys. Rev. Lett. **55**, 1327 (1985).
[12]M. Scheffler and U. Scherz, in *Proceedings of the 14th International Conference on Defects in Semiconductors, Paris, 1986* (Ref. 1), p. 353.
[13]M. J. Puska, O. Jepsen, O. Gunnarsson, and R. M. Nieminen, Phys. Rev. B **34**, 2695 (1986).
[14]C. Corbel, M. Stucky, P. Hautojärvi, K. Saarinen, and P. Moser, Phys. Rev. B **38**, 8192 (1988).
[15]K. Saarinen, P. Hautojärvi, P. Lanki, and C. Corbel, Phys. Rev. B **44**, 10 585 (1991).
[16]D. M. Ceperley and B. J. Alder, Phys. Rev. Lett. **45**, 566 (1980); we use their local exchange-correlation functional as parametrized by J. Perdew and A. Zunger, Phys. Rev. B **23**, 5048 (1981).
[17]D. R. Hamann, M. Schlüter, and C. Chiang, Phys. Rev. Lett. **43**, 1494 (1979).
[18]U. von Barth and C. D. Gelatt, Phys. Rev. B **21**, 2222 (1980).
[19]G. B. Bachelet, D. R. Hamann, and M. Schlüter, Phys. Rev. B **26**, 4199 (1982).
[20]L. Kleinman and D. M. Bylander, Phys. Rev. Lett. **48**, 1425 (1982).
[21]X. Gonze, P. Käckell, and M. Scheffler, Phys. Rev. B **41**, 12 264 (1990).
[22]R. Stumpf, X. Gonze, and M. Scheffler (unpublished).
[23]J. Ihm, A. Zunger, and M. L. Cohen, J. Phys. C **12**, 4409 (1979).
[24]H. Hellmann, *Einführung in die Quantenchemie* (Deuticke, Leipzig, 1937), p. 285; R. P. Feynman, Phys. Rev. **56**, 340 (1939).
[25]D. Vanderbilt, Phys. Rev. B **41**, 7892 (1990).
[26]K. Laasonen, R. Car, C. Lee, and D. Vanderbilt, Phys. Rev. B **43**, 6796 (1991).
[27]R. Car and M. Parrinello, in *Simple Molecular Systems at Very High Density,* edited by A. Polian, P. Loubeyre, and N. Boccara (Plenum, New York, 1989).
[28]G. Pastore, E. Smargiassi, and F. Buda, Phys. Rev. A **44**, 6334 (1991).
[29]*Handbook of Chemistry and Physics,* 62nd ed., edited by R. C. Weast (CRC, Boca Raton, 1988).
[30]Q-M. Zhang, G. Chiarotti, A. Selloni, R. Car, and M. Parrinello, Phys. Rev. B **42**, 5071 (1990).
[31]G. B. Bachelet and N. E. Christensen, Phys. Rev. B **31**, 879 (1985).
[32]S. G. Louie, M. Schhluter, J. R. Chelikowsky, and M. L. Cohen, Phys. Rev. B **13**, 1654 (1976).
[33]G. A. Baraff and M. Schlüter, Phys. Rev. B **30**, 3460 (1984).
[34]K. Laasonen and R. M. Nieminen (unpublished).
[35]K. Laasonen and R. M. Nieminen, J. Phys.: Condens. Matter **2**, 1509 (1990).
[36]C. Z. Wang, C. T. Chang, and K. M. Ho, Phys. Rev. Lett. **66**, 189 (1991).
[37]P. Hautojärvi, P. Moser, M. Stucky, and C. Corbel, Appl. Phys. Lett. **48**, 809 (1986).
[38]C. Corbel, F. Pierre, P. Hautojärvi, K. Saarinen, and P. Moser, Phys. Rev. B **41**, 10 632 (1990); C. Corbel, F. Pierre, K. Saarinen, P. Hautojärvi, and P. Moser, Phys. Rev. B (to be published).
[39]M. J. Puska and C. Corbel, Phys. Rev. B **38**, 9874 (1988).
[40]S. Mäkinen and M. J. Puska, Phys. Rev. B **40**, 12 523 (1989).